10-2023

Influence of Feedstock and Moisture Content in a Continuous Feed Screw Torrefier

Anna H. Partridge
Smith College

Isabella Casini
Smith College

Denise A. McKahn
Smith College, dmckahn@smith.edu

David Carter
California Polytechnic University

Charles Chamberlin
California Polytechnic University

See next page for additional authors

Influence of Temperature, Feedstock and Moisture Content in a Continuous Feed Screw Torrefier

Anna H. Partridge, Isabella Casini, and Denise A. McKahn

Picker Engineering Program, Smith College, Northampton, Massachusetts

David Carter, Charles Chamberlin, Arne Jacobson*, Kyle Palmer, Yaad Rana, and Mark Severy

Schatz Energy Research Center, California Polytechnic University Humboldt, Arcata, California

Abstract

This paper investigates the parameters impacting product quality in a pilot scale biomass torrefaction reactor. The system analyzed in this work was designed and manufactured by Norris Thermal Technologies for use in Big Lagoon, California at a remote mill site. The torrefaction unit was a continuous feed reactor with an electrically heated screw, which served the dual purpose of heating and biomass conveyance. The energy and mass yields were found to be highly correlated in this analysis. The best predictor of both energy and mass yield in this study was the steady state temperature measurement in the biomass product closest to the outlet of the reactor. The variation in residence time, moisture content and feedstock species are not statistically significant parameters for predicting mass yield or energy yield. The enhancement of the higher heating value was correlated with temperature and species with the enhancement factor greatest on average for tan oak, next largest for slash and redwood, and smallest for douglas fir. The proximate analysis exhibited a strong correlation between both fixed carbon and volatile matter and mass yield, as well as a moderate correlation to the product 3 steady state temperature. The ash content of the product did not exhibit a correlation with mass yield or temperature. The residence time, feedstock moisture content, and feedstock did not have statistically significant effects on the proximate analysis content when mass yield and temperature were considered.

Keywords: biomass, bioenergy, product quality, proximate, torrefier, ultimate

1. INTRODUCTION

Biomass residues from forestry operations that are determined to be economically unviable for post-processing in wood industries are left on hillsides to decompose or burn in controlled piles. These biomass residues represent an untapped energy source which can be used to produce electrical and thermal power in a renewable way. Because plant matter is abundantly distributed around the world, bioenergy conversion demonstrates large potential for use on a wide-scale with a low carbon footprint [1].

There are multiple ways to convert solid biomass into fuel and further convert the fuels into thermal and electrical energy. The most common types of biomass energy conversion strategies rely on biological processes, combustion, gasification, torrefaction and/or pyrolysis. Though each process produces a different type of fuel, their integration with existing thermal and electrical generators depends on the consistency and predictability of the fuel characteristics and quality. This work focuses on torrefaction.

Biomass torrefaction and pyrolysis refer to heat treatment at temperatures below combustion in the absence of oxygen to produce primarily solid and liquid fuel. Pyrolysis takes place between 400-700°C at ambient pressure [2], while torrefaction takes place at lower temperatures between 200-300°C [3, 4, 5]. Pyrolysis can take place in either slow pyrolysis or fast pyrolysis processes, characterized by long residence time between 5-30 minutes at temperatures near 400°C, and short residence time between 1-20 seconds at 500°C respectively [2]. Fast pyrolysis requires small particle sizes, while slow pyrolysis can utilize relatively larger solids [2]. Pyrolysis primarily produces liquid bio-oil which can be utilized in the production of chemicals, upgraded motor fuel, and electricity [2].

Torrefaction is a form of mild-pyrolysis in which the biomass is dried and some of the volatile matter is vaporized, reducing the mass more than the energy content and thus resulting in an increased energy density in the solid product. Residence times of biomass inside a torrefaction reactor can range from a few minutes to 3 hours [6]. The solid fuel has substantially improved grindability, and when combined with pelletization, the energy density can be increased further, reducing transportation and storage costs [5]. Additionally, the solid fuel is less prone to biological degradation, allowing long term storage in both dry and humid locations [5]. The gas produced contains primarily CO, CO_2, H_2 and a small amount of methane, and can contain detectable amounts of toluene, benzene and other hydrocarbons [1]. This gas can be recovered and used as a fuel source for heating or electricity production, though the low heating value

*Corresponding author email address: dmckahn@smith.edu

of the gas limits the extent of these applications [1]. The liquid fraction of the product is generally composed of the condensed water vapor, acetic acids, alcohols, aldehydes and ketones [1]. Biomass processed in a torrefaction reactor, or torrefier, can produce a solid fuel which can serve as a substitute for coal in thermal power plants and metallurgical processes [1].

Torrefaction can be performed in a Thermogravimetric Analyzer (TGA) [4, 7, 8] or in small scale batch reactors [9, 10]. Direct heating is common in batch torrefaction processes, in which a hot inert gas such as nitrogen is used in fluidized bed torrefaction reactors to suspend the biomass particles. This particle suspension allows for enhanced convective heat transfer from the gas to the solid wood [11]. Grigiante et al. [12] performed experiments using direct heating to determine the impact of temperature and residence time on mass yield, and evaluate mass yield as a primary indicator of product quality and properties, independent of thermal pathway. Kim et al. [9] used a batch reactor to determine the higher heating value and mass loss for Acacia and Albasia wood species. While the conditions in batch processes can be controlled more precisely, the reactors are not economically viable for biomass energy pretreatment due to the small feedstock processing rates. Reactors which can continuously move large quantities of biomass through a heated reactor are necessary for implementation of torrefaction on a large scale. Reactor types, moving bed reactor design, and design tradeoffs are well articulated in [13], along with the modeling of mass and heat transport mechanisms.

The product characteristics for continuous pilot scale reactors have been recently discussed [14], [6], [15], and [16]. Each of these experiments used screw conveyance to move the biomass continuously through a heated reactor for a specific residence time, while the feedstock used in the Strandberg et al. [6] experiment was dry chipped stem wood from Norway spruce grown in Northern Sweden, Shang et al. [15] used pine wood chips from Zealand, Denmark, Keivani et al. [16] used red pine in Turkey. In continuous pilot scale reactors, the most common method for heating biomass is external reactor heating using electric heaters.

Strandberg et al. [6] performed a continuous torrefaction experiment using a pilot scale rotary drum reactor heated by five external electric heaters. Nachenius et al. [14] used a two externally heated reactors in series. Each reactor was heated by three independently controlled electrical heaters and temperature readings were taken of the biomass by four screw mounted thermocouples [14]. Another method of indirect heating used in continuous torrefaction processes is circulated heated fluid such as gas from petroleum burning[15, 17] or using screw conveyance surrounded by a temperature controlled furnace [16]. Continuous nitrogen flow was used to maintain an inert (non-combusting) atmosphere in both TGA batch experiments and continuous torrefaction reactors [14, 6, 15, 18, 12, 16].

Strandberg et al. [6] varied the residence time between 8 and 25 minutes, and temperatures between 260 and 310°C. This paper quantifies the higher heating value, ultimate analysis, proximate analysis, milling energy (a measure of grindability), angle of repose (an indirect measure of feedability), contact angle and equilibrium moisture content (a measure of hydrophobicity) [6]. They found that increased torrefaction severity increased the hydrophobicity, carbon fraction and higher heating value and decreased the milling energy, angle of repose and volatile matter.

Nachenius et al. [14] manipulated four parameters: reactor temperature, reactor residence time, degree of filling of the reactor, and the nitrogen purge gas flow rate. The experiment measured spacial distribution of internal temperature, product yields, proximate analysis and grindability. This paper demonstrated that torrefied biomass properties could be reasonably accurately predicted using linear correlations given the mass yield of the experiment. Additionally, they reported that the temperature and residence time had a greater impact on the product characterization that nitrogen flow rate or degree of filling of the reactor. Shang et al. [15] developed a two step kinetic model of continuous torrefaction in a pilot scale torrefier. All wood chips used in this study were pine with a moisture content of 16% on a wet basis. The kinetic model predicted reasonably well the mass yield and higher heating value of samples obtained from residence times of 1 hour based upon the temperature profile of the biomass inside the reactor.

There have been limited works utilizing the specific species of wood that are native to Northern California, despite the vast forestry industry in Northern California and the Pacific Northwest. Additionally, there is a gap in the literature on the topic of continuous feed reactors which use internal screw heating rather than external electrical or fluid jacketed methods for heating. The majority of the work that has been done on continuous reactor torrefaction has used dry feedstock, or feedstock at a fixed moisture content, however, often wood waste from forestry residues does not have consistent moisture content.

Electrical resistance heaters have previously been used for biomass heating through torrefaction reactor walls. This work characterizes the temperature profiles of an electrically heated screw conveyor that directly heats biomass through conduction with the solid electrified screw. The screw also serves as a conveyance mechanism for maintaining continuous flow of biomass through the reactor at all times. The mass flow rate through the system and the thermal profiles in time and space are characterized for this unique heated conveyance device.

The focus of this work is to provide an analysis of the parameters which can be used to control the product characteristics of biomass in a torrefaction reactor. This torrefier was installed and operated in conjunction with the Waste to Wisdom project, part of the Biomass Research and Development Initiative, funded by the U.S. Department of Energy (DE-EE0006297), as described in [19]. Initial test results were provided in [20], with a detailed evaluation of specific electricity demand, torrefied briquette grindability, briquette volumetric energy density, and briquette durability. A detailed evaluation of residence time associated with the biomass solid mass transport through the screw conveyor were presented in [21]. The correlations between solid input and output characteristics explored in this work provide a basis for future work on continuous torrefaction using heated screw conveyance. The data collected as a part of this research included information about variation in the feedstock species and moisture content, as well

as the controllable parameters of the torrefaction reactor itself, including temperature set point and residence time. Feedstocks tested in this study included douglas fir, redwood, tan oak, and hardwood "slash," a combination of tan oak and other unfiltered hardwood with bark and branches. The product characteristics studied were the torrefied solid mass yield, an indicator of the severity of torrefaction, the energy yield of the process, the enhancement of the wood's higher heating value from inlet to outlet (enhancement factor), the proximate analysis of feed and product, as well as model predictions of elemental composition.

2. EXPERIMENTAL HARDWARE

The torrefaction reactor in this study is a pilot scale Biogreen® unit manufactured by Norris Thermal Technologies in partnership with the French company ETIA, pictured in Figure 1. The reactor and system control and monitoring equipment was built on a trailer bed in order to allow for easy transportation to remote locations. The torrefaction system included the torrefaction reactor itself, a tube and shell condenser for collecting liquid bio oil and water vapors from the torrefaction product gas (torrgas), a water jacketed cooling auger for the solid torrefied product, and a thermal oxidizer for converting the noxious torrgas products into combustion products.

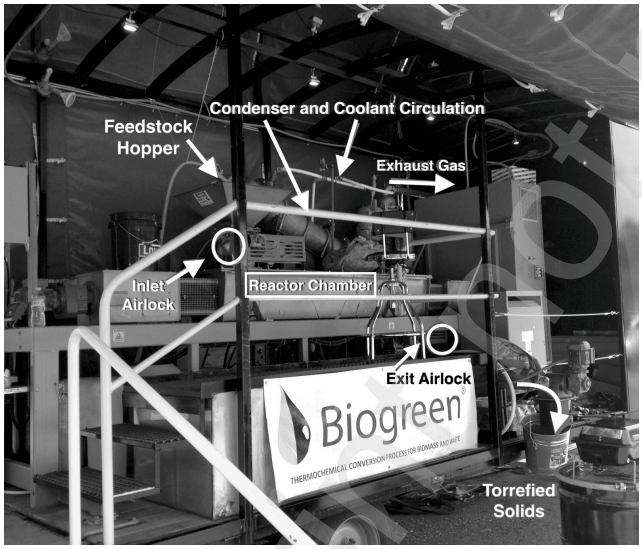

Figure 1: Front view of the torrefaction reactor on portable trailer.

In Figure 2, following the path of the biomass, raw feedstock entered the hopper indicated by the boxed number (1) and passed through the rotating airlock vanes (2) into the main torrefaction reactor (3). The airlock rotation rate was controlled by adjusting the motor frequency, and corresponded to the intended residence time of the biomass in the reactor, in order to manage the fill level of chips in the torrefier. Solid torrefied product exited at the outlet airlock (5) into the cooling auger (6), a cold water jacketed chamber which reduced the temperature of the biomass to ambient temperature. The cooling auger was

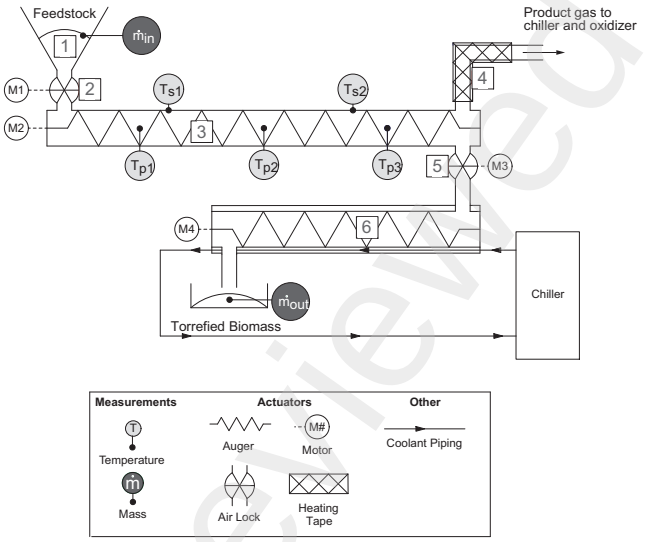

Figure 2: Modified P&ID diagram with relevant measurement locations and torrefier components labeled.

open at the outlet, and therefore contained air at atmospheric conditions.

As biomass moved down the length of the torrefaction chamber, water vapor and torrgas evolved, and left through an insulated pipe at the far end of the reactor (4). The gas constituents were pulled by a fan through a tube and shell condenser, and liquid products were collected at the base of the condenser. The water used to cool the condenser and the cooling auger were recirculated through a mechanical chiller. After the condenser, the gas passed through a particulate filter. After the torrgas passed through the filter, the thermal oxidizer (10) introduced excess air to the gas mixture at temperatures near 700^oC. This oxidation resulted in conversion of dangerous carbon monoxide constituents into less harmful carbon dioxide emissions. The hot combustion products from the thermal oxidizer were either vented to the atmosphere or introduced into the Beltomatic dryer for biomass pre-drying at temperatures around 400^oC. The torrgas pathway downstream of the torrefier is not shown in Figure 2 and is not the subject of this study.

The torrefaction reactor was heated through the electrically conductive metal Spirajoule® screw. The screw had an approximate radius of $3.63in$ and served the dual purpose of heating and moving the biomass down the length of the reactor. The stainless steel frame of the reactor was insulated on all surfaces with ceramic insulation to minimize heat loss to the ambient.

Type K thermocouples were used to continuously monitor the spatial distribution in temperature inside the reactor along the biomass transport pathway. Two thermocouples, referred to as 'sky' thermocouples and designated with the subscript s in Figure 2, were placed along the top of the reactor to measure gas temperatures. Three thermocouples, called 'product' thermocouples and designated with the subscript p in Figure 2, were placed in one of the side walls of the reactor, approximately one screw radius above the bottom of the reactor in order to ensure the rotating screw did not dislodge the probes. As shown in Figure!3, the probes extended slightly past the torrefier wall in

order to measure the temperature of the biomass at that location.

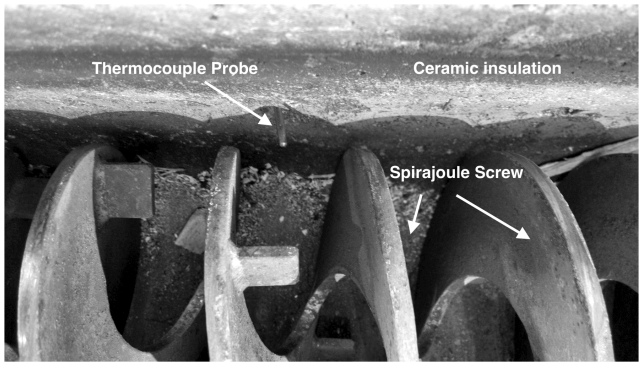

Figure 3: View of the internal screw from above with product thermocouple probe visible.

The control panel allowed the operator to choose when to purge the reactor chamber with nitrogen to maintain an inert gas atmosphere. After each purge, the nitrogen was released from a pressurized tank for approximately 30-45 seconds.

Feedstock mass supplied to the reactor, m_{in} was measured by taking the difference in mass between full and empty buckets as the chips were loaded into the hopper, and $\dot{m}_{in}$ was determined on an average basis for each run by dividing the total mass added to the hopper by the total time the inlet airlock was open and feeding mass.

Solid product mass produced at time i, $m_{out,i}$, was periodically recorded at the outlet of the cooling auger by measuring mass in buckets and subtracting the bucket tare weight every 2 minutes. Total mass of the torrefied wood chips produced in a run, m_{out}, was calculated as the sum of all incremental solid mass out data collected during the run. The incremental solid product mass flow rate out, $\dot{m}_{out,i}$, was then calculated for each time interval, $(t_i - t_{i-1})$, as

$$\dot{m}_{out,i} = \frac{m_{out,i}}{(t_i - t_{i-1})}. \quad (1)$$

The incremental mass flow rate was not averaged over the course of the run because the start up and shutdown mass flow profiles were not consistent. The incremental mass flow rate was used to approximate the start of steady state operations during each run. A full characterization of the torrefier residence times can be found in [21].

3. EXPERIMENTAL PARAMETERS AND BIOMASS CHARACTERISTICS

In this section the feedstock characteristics and state variables are presented. The variables in this study were the feedstock species, moisture content of the feedstock, residence time in the torrefier, and torrefier set point temperature, T_{spj}. Table 1 details the combinations of input parameters that were tested in each individual experimental run. A description of, and the rationale for, the range of values or categories for each variable is provided in the following subsections. The first column in Table 1 notes the run number. Consecutive experimental tests were conducted over a period of several days.

3.1. Biomass Feedstock

In this study, four different woody biomass feedstocks were used as the raw input to the torrefaction reactor. Each feedstock is native to Northern California. The feedstock arrived to the site as chipped wood, which was sorted into piles by species type: tan oak, douglas fir, redwood, and hardwood slash. The douglas fir chips did contain the top part of the tree which is usually left unprocessed on the hillside, but did not contain branches or bark. The composition of the hardwood slash was primarily tan oak with bark and other impurities.

The feedstock was sorted by size on one of two mechanical screeners. The hardwood slash, and the majority of the tan oak and douglas fir chips were sorted using a large DS6162 Peterson deck screener to a tolerance of less than or equal to 0.375 inches as the largest dimension. The redwood was screened by a custom screener to a tolerance of less than or equal to 0.5 inches as the largest dimension.

3.2. Moisture Content

In order to create variability in the moisture content of the feedstock, portions of the piles after screening were fed through a Beltomatic dryer manufactured by Norris Thermal Technologies. The dryer used hot exhaust gases from the torrefaction reactor to dry the chipped wood to moisture contents in the range of 3-15% by mass on a wet basis. Because the tan oak fines sorted on the deck screener contained dust particles, passing the deck screened hardwood through the dryer posed an increased fire hazard. Therefore, the tan oak, hardwood slash, and douglas fir chips sorted on the deck screener were spread across the concrete site in a thin layer no more than 6 inches deep to dry in the sun for multiple days, reducing the moisture content to approximately 10%.

Moisture content of the feedstock was measured at the beginning of each experimental run. Moisture content measurements of the torrefied wood product were taken immediately after each run. A Veritas i-Thermo Moisture Analyzer was used to take these moisture content measurements on a wet mass basis. To take the measurements, a halogen lamp heater was used to preheat samples to 103^oC, a sample of biomass of approximately $5g$ was loaded onto the pan and the automatic, continuous mass measurement began. The device was programmed to stop taking measurements when the change in mass lost was less than 0.1% in 1 minute. The average moisture content of three feedstock buckets was used as the moisture content of the feedstock, μ_{in}, while the average between two samples of torrefied biomass produced were used to represent the average moisture content of the torrefied wood product, μ_{out}.

3.3. Residence Time

The residence time is an indication of how long the wood chips spend in the reactor after entering the inlet airlock before they are rotated out of the exit airlock. In [21], a tracer

Table 1: Experimental test matrix for pilot scale torrefier with variable feedstock, moisture content (MC), temperature (Temp.) and residence time (t_r).

Run	Temp.	t_r	Feedstock	MC
15	300^{o}C	6 min	douglas fir	6.1%
35	300^{o}C	6 min	redwood	3.4%
36	300^{o}C	6 min	redwood	31.6%
22	300^{o}C	6 min	hardwood slash	7.6%
27	300^{o}C	6 min	hardwood slash	10.7%
17	300^{o}C	8 min	douglas fir	12.9%
41	300^{o}C	8 min	redwood	4.9%
40	300^{o}C	8 min	redwood	5.2%
38	300^{o}C	8 min	redwood	9.2%
39	300^{o}C	8 min	redwood	17.5%
23	300^{o}C	8 min	hardwood slash	6.7%
28	300^{o}C	8 min	hardwood slash	11.2%
30	300^{o}C	8 min	tan oak	10.4%
9	325^{o}C	6 min	douglas fir	9.4%
14	350^{o}C	6 min	douglas fir	3.7%
8	350^{o}C	6 min	douglas fir	4.4%
16	350^{o}C	6 min	douglas fir	11.6%
5	350^{o}C	6 min	douglas fir	26.3%
24	350^{o}C	6 min	redwood	7.5%
25	350^{o}C	6 min	redwood	26.1%
20	350^{o}C	6 min	hardwood slash	6.8%
26	350^{o}C	6 min	hardwood slash	10.6%
11	350^{o}C	6 min	tan oak	6.8%
12	350^{o}C	6 min	tan oak	7.3%
13	350^{o}C	6 min	tan oak	15.3%
31	350^{o}C	8 min	douglas fir	4.6%
19	350^{o}C	8 min	douglas fir	11.6%
32	350^{o}C	8 min	tan oak	4.3%
29	350^{o}C	8 min	tan oak	11.2%
7	400^{o}C	6 min	douglas fir	5.2%
10	400^{o}C	6 min	douglas fir	6.4%
34	400^{o}C	6 min	douglas fir	10.1%
6	400^{o}C	6 min	douglas fir	22.3%
21	400^{o}C	6 min	hardwood slash	6.0%
33	400^{o}C	6 min	tan oak	5.0%
37	400^{o}C	6 min	tan oak	11.6%

study was conducted with this torrefier to determine the relationship between the measured time the chips spent in the reactor and the residence time set point. The residence time set on the programmable logic controller (PLC) was found to approximate the ideal residence time, however, on average the measured residence time was 7% longer than the nominal or set point residence time [21]. In this work, all reported residence times are the set-points, as the individual residence times were not measured while the torrefier was actively heating the material. The residence time was set by the torrefier operator on the control panel and the PLC software converted the desired residence time into a frequency set point for the screw motor. The two residence times used for this study were 6 minutes and 8 minutes.

3.4. Temperature Regulation

The temperature in the reactor was controlled by setting the desired screw set point temperature on the PLC panel. An ungrounded thermocouple measured the temperature of the Spirajoule® screw, and a PID control algorithm was used to maintain a set point temperature within approximately 5^oC of the set point, $T_{spj,set}$ at all times. The dynamic thermal response will be further described in Section 4. The Spirajoule® screw set point temperatures used in the experimental runs were 300^oC, 325^oC, 350^oC and 400^oC.

3.5. Product Characterization Metrics

The higher heating value, HHV, of both the raw biomass feedstock, HHV_{fs}, and torrefied wood product, HHV_{prod}, for each run was measured off-site at the Schatz Energy Research Center in Arcata, California using a Parr Instruments bomb calorimeter. Biomass samples were blended into fines and placed into an over at 105^oC for 24 hours to evolve all water. The instrument was calibrated using benzoic acid. During operation, oxygen was used as the pressurized gas. All mass measurements were taken with an accuracy of +/-0.001g.

Additional calculations to find mass yield and energy yield utilized the higher heating value, moisture content and mass input and outputs measured during the experimental runs and will be further described in Section 5. The bulk density of the feedstock was measured at the field site before each run following standard method CEN/TS 15103: “Solid Biofuels: Methods for the determination of bulk density”.

4. THERMAL RESPONSE

This section details both the thermal response of the torrefier during a typical experimental run as well as the process used to estimate the steady-state temperature profiles.

4.1. Typical Dynamic Response

A typical experimental run involved initially warming up the reactor by supplying power to the Spirajoule® screw (location M2 in Figure 2), then injecting feedstock into the reactor through the inlet hopper (location 1). The feedstock was then in direct contact with the heated screw as it moved through

the reactor. The heat supplied to the Spirajoule® screw was controlled with a PID controller to maintain a desired setpoint temperature as explained in Section 3. It is important to note that the setpoint temperature of the Spirajoule screw will not be equal to the temperature of the biomass or the evolving gases. The temperature measurements change in space, along the length of the reactor, and in time throughout the course of the run. During an experiment, biomass enters the reactor, entrained water and product gases, called torrgases, evolve, and solid product torrefied wood leaves. Due to constant heat input along the length of the screw at any given time, the product mass is expected to increase in temperature along the length of the reactor.

In each experimental run, the temporal and spatial profiles followed a similar trajectory. Run 29 has been chosen as an example of a typical experimental run, in which the temporal and spatial profiles follow the overall trajectories seen throughout the many experiments conducted. Figure 4 shows the temperature trajectories for all thermocouple measurements over the course of a single run. Prior to the beginning of the experimental run, the reactor was preheated to the initial temperatures that are shown at time $t = 0$ in Figure!4. The thermocouple measurements are labeled according to their location in the upper "sky" section, denoted with a subscript s, or the lower "product" section, denoted with subscript p. Thermocouples are numbered sequentially according to their distance from the inlet, with the label "1" corresponding to the thermocouple probe closest to the feedstock hopper and numbers increasing by integer amounts as they move further from the hopper.

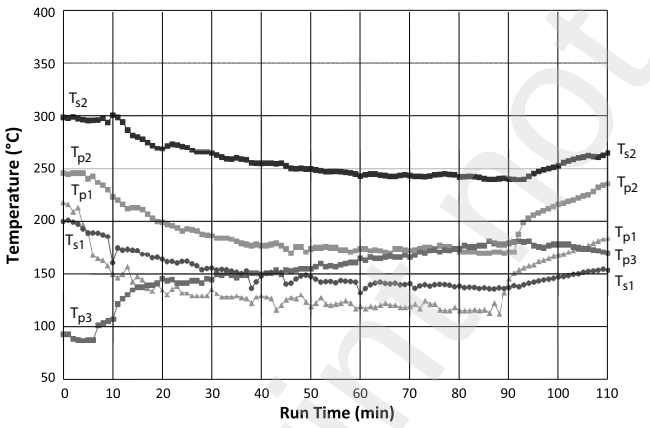

Figure 4: Temporal thermal profile inside the torrefaction reactor during run 29 with tan oak at set point 350°C for an 8 min residence time. T_{pi} indicates the product temperatures at locations $i = 1$, 2, or 3, and T_{si} indicates the gas temperatures at location $i = 1$ or 2.

The inlet airlock is opened with the hopper full at time $t = 0$ min, introducing biomass into the reactor. After the initial injection of biomass, the resultant decrease in temperature is clear for all the thermocouples except T_{p3}. The first two temperatures to respond to the introduction of mass are T_{s1} and then T_{p1}, the two locations closest to the inlet. These two temperatures begin to decrease, as the ambient temperature biomass comes in contact with the hot reactor materials, including the heated screw.

While the first two thermocouples respond almost immediately to the injection of biomass, which is not surprising given their proximity to the hopper, the second product thermocouple, T_{p2}, responds later, at around $t = 5$ min. The last thermocouple to respond is T_{s2} which starts decreasing in temperature at around 10 minutes. Because a biomass chip is expected to take, on average, 8 minutes to move from the inlet to the outlet of the reactor due to its target residence time, these differences in the temporal temperature responses follow an expected trajectory. The third product thermocouple, T_{p3} sees an increase in temperature between $t = 7$ min and 13 min, and then a slower, but steady increase for the remainder of the run. The rapid increase in temperature toward the beginning of the run is likely caused by hot biomass reaching the last third of the reactor during its 8 minute residence time, while the steady, lower rate of increase for the remaining run time indicates that the temperature on the last third of the reactor is shifting towards equilibrium with the biomass and the adjacent portions of the reactor. One possible explanation for the unique T_{p3} trajectory is ambient temperature air being introduced into the reactor through the outlet airlock vanes and cooling the reactor temperature at the outlet below the average internal temperature. Further thermal modeling efforts have illustrated this possibility and are under investigation [22].

The first solid product exited the torrefier at $t = 9$ min after the beginning of the run, and the first solid product mass flow was measured at the outlet of the cooling auger at time $t = 10$ min. The mass flow stabilizes by time $t = 20$ min and the mass flow rate fluctuated between 45 and 60 g/min for over one hour of steady state flow, with the last steady state mass flow of biomass exiting the cooling auger between 90 and 100 minutes into the run.

At time $t = 88$ min, the inlet airlock was turned off, stopping the flow of biomass into the reactor. However, the screw continues to force biomass out of the torrefier. For the remainder of the run, the temperatures of all thermocouples with the exception of T_{p3} are increasing, as the metal screw begins to heat the gas and ceramic insulation to higher temperatures in the absence of biomass. The product 1 and 2 thermocouples show sharp increases in temperature, as these change from measuring solid biomass temperature to empty reactor gas temperatures. Sky thermocouples exhibit a less dramatic increase in temperature as the biomass leaves the reactor, and product 3 shows a similarly slow rate of decline in the last minutes of the experimental run. Experiments performed by [14] indicate a similar trajectory for the last product thermocouple.

4.2. Steady-State Temperature Profiles

To examine the influence of temperature on product characteristics and input parameters, an indication of reactor temperature for each experiment was necessary. The experiments were characterized by their steady state (SS) temperatures, $T_{p1,SS}$, $T_{p2,SS}$, $T_{p3,SS}$, $T_{s1,SS}$, and $T_{s2,SS}$, where the subscripts s and p indicate sky temperature and product temperature respectively, and numbers correspond to location as described in Section 2.

The steady state temperature was determined for each run by a careful analysis of the thermal profile and the outlet solid product mass flow rate over each individual run. Because the length of the run, thermal trajectories and mass flow trajectories varied between experiments, a simple algorithm for determining steady state could not be created. Instead, determination of steady state was done manually on inspection of the mass and thermal profiles.

As temperatures reached steady state toward the end of each run, analyzing the temperature profiles for a steady state window was done starting from the end of the run, rather than the beginning. The residence time in the torrefier did not exceed 8 minutes for any run, and measurements of mass flow were taken every two minutes. Therefore, 10 minutes before the last steady state mass flow data point was chosen to designate the endpoint of internal steady state operations. For example, if mass flow rate began to decrease at $t = 90$ min, $t = 80$ min was chosen as the endpoint for internal steady state, in order to ensure that biomass flow had not begun to decrease inside the reactor. After choosing this endpoint, the temperature profiles in the 10 minutes prior to the endpoint were examined to ensure that there were no unusual patterns in the mass flow or thermal profiles. Common unusual patterns in mass flow data were considered to be fluctuations of greater than ± 10 g, often indicating cooling auger blockage, while the thermal profiles were examined for unexplained deviations of ± 8^{o}C from average temperature during the 10 minute time window. If no unusual data trends existed, then the temperatures for the ten minutes before the previously determined endpoint were averaged for each thermocouple and recorded as the steady state temperatures. If inconsistencies in mass flow data or unexplained outliers in the temperature measurements were found, the endpoint was shifted earlier in the run, just before the inconsistency occurred, and the prior ten minutes were deemed to be indicative of steady state temperature under the previously described criteria.

Steady state reactor temperature changes in space along the length of the torrefier, as seen in Figure 5. Additionally the runs with the same Spirajoule® set point temperatures are clustered around the setpoint. The expected temperature profiles with consistent energy input would indicate continuous temperature increase along the length of the torrefier as the biomass increases in sensible heat, water is evaporated and the gases are evolved from the biomass torrefaction reactions. This thermal trajectory was measured by [15] in a closed system batch reactor. However, the mechanical processes of filling and emptying the biomass introduce sources of cooler air into the reactor process and chemical reactions, that cause unpredictable differences from the expected trajectory.

The temperature distribution in Figure 5 does show an overall increase in temperature as biomass travels the length of the torrefier. A notable exception to this distribution is the temperature reading closest to the outlet, T_{p3}. Additionally, between product 1 and sky 1, there is usually an increase in temperature, although 8 runs out of 36 show a decrease in temperature between these two thermocouples. The T_{s1} and T_{s2} thermocouples are located 3.75 inches apart, and therefore are expected to read similar temperatures, however it is likely that because the sky 1 thermocouple probe is reading gas temperatures and the product 1 thermocouple is in contact with the biomass solids, these temperatures are measuring different thermal dynamics. For these 8 runs, the exhibited decrease in temperature was not correlated with the Spirajoule® set point temperature or the residence time.

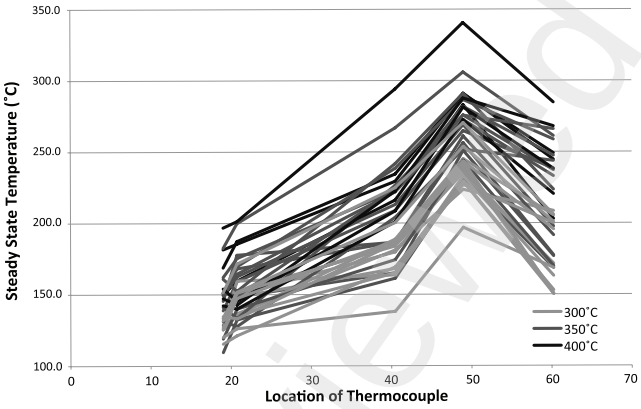

Figure 5: Steady state temperature distribution along the length of the torrefier measured using external dimensions shown in Figure 2. All runs are grouped by their Spirajoule® set point temperature, $T_{spj,set}$.

As shown in Figure 5, there is an overall increase in temperature between product 1, product 2 and sky 2 thermocouples throughout all runs, regardless of Spirajoule® temperature set point. The product 3 temperature measurement is also consistently lower than the sky 2 temperature across all product runs, but the magnitude of the difference between sky 2 and prod 3 is inconsistent between runs, with an average decrease of 52.2^{o}C from sky 2 to product 3 thermocouples, and a standard deviation that is nearly half of the average difference, at 23.0^{o}C. The product 3 thermocouple may measure lower temperatures than the second sky thermocouple due to airflow leaking into the reactor at the exit airlock. This airlock is closer to the fan which draws gases out of the reactor. Gaps between the airlock vanes and the wall of the airlock would allow ambient air to flow into the reactor due to the slight negative pressure created by the fan. Additionally emptied vanes filled with only ambient temperature air rotating into the reactor would cause a drop in temperature in the last third of the torrefier, which could cool the biomass as it passes the product 3 thermocouple. A separate thermal modeling effort is focused on determining whether the air leak in the outlet airlock could also impact the spatial temperature distribution upstream.

Figure 6 shows the standard deviation for each thermocouple steady state temperature measurement at three different Spirajoule® set point temperatures, 300^{o}C, 350^{o}C and 400^{o}C. The inconsistency in the product 3 thermocouple reading does not end with its unexpected thermal trajectory. The product 3 temperature measurement also has the highest standard deviation for runs with a Spirajoule® set point of 300^{o}C and 350^{o}C, and the second highest standard deviation for runs at Spirajoule® set point of 400^{o}C, as shown in Figure 6. This in-

dicates that there is more variability in the temperature at steady state in the final third of the reactor, nearest the outlet, regardless of the temperature set point.

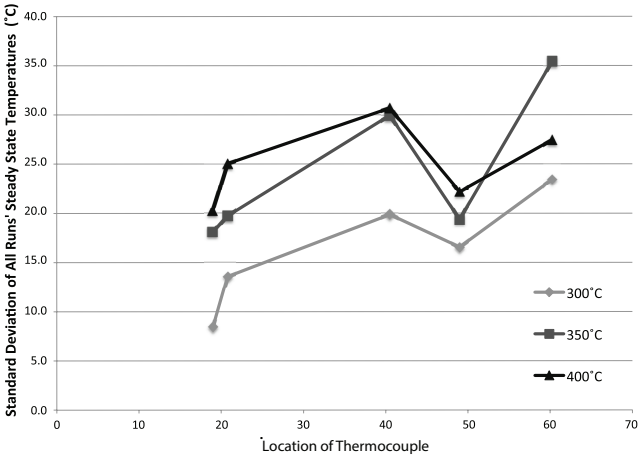

Figure 6: Standard deviation in the steady state temperature measurements across all runs. These data are grouped by Spirajoule® set point temperature, $T_{spj,set}$, as a function of location along the external length of the torrefier.

The sky 2 temperature measurements have a lower standard deviation than the sky 1 measurements for both runs at 350^{o}C and 400^{o}C, suggesting that airflow or deviations in ambient temperature of the input biomass from the inlet airlock may influence the variability in the gas temperatures closest to the inlet. Besides the lower standard deviation of the sky 2 thermocouple, the standard deviations within each temperature group generally increase as the product moves through the reactor in space, indicating that the variation in temperature profiles between runs at the same set point temperature is increasing as the product undergoes the torrefaction chemical reactions. Additionally, for all data excluding T_{p3} measurements at 400^{o}C, Figure 6 shows that as the temperature set point increases, there is a general increase in standard deviation for each thermocouple measurement, possibly caused by the increasing complexity of the chemical reactions taking place as the degree of torrefaction increases.

5. MASS AND ENERGY YIELD

As solid biomass is heated, the torrefaction reaction evolves gas from the hemicellulose and lignin components of the wood [23], producing gaseous products and reducing the overall mass of the solid wood. As a result the mass yield for each torrefaction experimental run can be used as measure of the extent of the torrefaction reactions, with decreasing mass yields indicating an increasing degree of torrefaction experienced by the biomass [14]. The mass yield, Y_m, is calculated on a dry basis as

$$Y_m = \frac{m_{out}(1-\mu_{out})}{m_{in}(1-\mu_{in})} \tag{2}$$

where m_{in} is the total solid mass (g) added to the hopper inlet during the course of the run, including before, during and after steady state was achieved, μ_{in} represents the average moisture content of the feedstock, unitless on a dry basis. The total solid mass output (g) and average moisture content of the product are represented by m_{out} and μ_{out} respectively.

The energy yield of each run is a measure of how much of the total energy content of the biomass feedstock is converted to solid energy dense torrefied product on a dry basis. The solid energy yield, Y_e, is calculated as

$$Y_e = Y_m \frac{HHV_{prod}}{HHV_{fs}} \tag{3}$$

where HHV_{prod} and HHV_{fs} represent the higher heating values (MJ/kg), of the product and feedstock respectively on a dry basis.

The mass and energy yield data exhibit a strong linear correlation that follows the data reported in the literature collected in other continuous torrefaction experiments performed by [14] and [6]. Figure 7 shows the solid energy yield plotted as a function of solid mass yield on a dry basis.

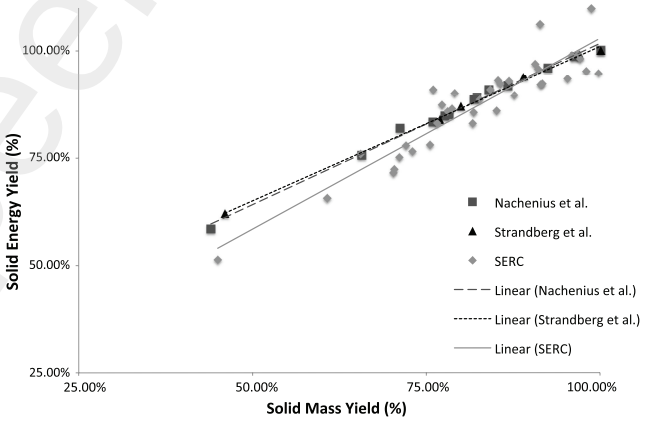

Figure 7: Yield ratio from three different continuous torrefaction experiments including Nachenius et al. [14], Strandberg et al [6] and this work's data, SERC. Linear trend lines for each data set have been superimposed on this figure

A 95% confidence interval for each linear regression slope was performed and the results are tabulated in Table 2. It was found that the confidence intervals for all three data sets overlapped, demonstrating that it is possible that the values of the slopes of the yield ratio data collected in these three different locations in different reactor types are equal. Though these experiments were performed in different types of continuous feed reactor and with different feedstocks, the relationship between mass and energy yield remains relatively consistent across experiments. There is always a linear relationship between mass yield and energy yield, due to the functional dependence of Y_e on Y_m in Equation 3.

To further investigate the influence of the mass yield on the energy content alone, and the influences of other variables on the energy content of the torrefied biomass, the enhancement factor, EF, calculated by Equation 4, was used as a metric of increased energy density. The enhancement factor is a mea-

Table 2: Confidence intervals with lower bound (LB) and upper bound (UB) for linear regression slopes for mass yield vs. energy yield in three different continuous torrefaction experiments.

Source	Regression Slope	LB	UB
Nachenius et al. [14]	0.718	0.708	0.792
Strandberg et al. [6]	0.718	0.671	0.766
SERC	0.888	0.765	1.012

sure of the percentage increase in higher heating value between the dry biomass coming into the torrefier and the dry product leaving the reactor [1]. Considering higher heating value as an indicator of energy content in the biomass, it follows that the enhancement factor,

$$EF = \frac{HHV_{prod}}{HHV_{fs}}, \tag{4}$$

is a measure of the increase in utility of the wood product.

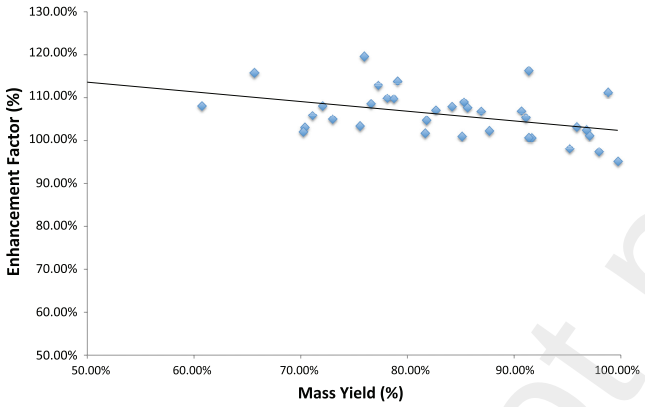

Figure 8: Enhancement factor as a function of solid mass yield for torrefied biomass samples collected by SERC.

The enhancement factor is weakly negatively correlated with mass yield, with a slope of -0.227 and an R^2 value of 0.212, as seen in Figure 8. The 95% confidence interval for this slope does not include zero, so although the correlation is weak and mass yield explains only 21.2% of the variation in the EF values, the slope is statistically significantly different from zero. This demonstrates that generally as the mass yield increases, the improvement in higher heating value of the wood from inlet to outlet decreases.

Multiple linear regression models were created for mass yield, energy yield and enhancement factor to determine the impacts of the controlled variables, moisture content, feedstock, temperature and residence time on the product characteristics. In order to determine the variables impacting the mass yield, a multiple linear regression model was created with input parameters of residence time, input moisture content, μ_{in}, feedstock, and each of the steady state temperatures, $T_{p1,SS}$, $T_{p2,SS}$, $T_{p3,SS}$, $T_{s1,SS}$, and $T_{s2,SS}$ individually. Spirajoule® set point temperature was not included in the variables due to the dependencies between set point temperature, preheat and steady state temperatures for all thermocouples. Additionally, only one temperature was considered in the multiple linear regression model at a time due to the dependencies between each temperature reading and the other temperatures in the reactor. Using the results of the multiple linear regression, the variable with a correlation co-efficient with the highest p value was eliminated and the regression was run again until all variables were statistically significant at an α level of 0.05. This process was used 5 times, once for each temperature measurement location.

The final multiple linear regression model for mass yield in each case simplified down to a single linear regression, with only the steady state temperature as a statistically significant variable. The regression equation with the highest R^2 value was determined to be the best predictor of the mass yield, and is described by Equation 5, where predicted mass yield, $\hat{Y}_m$, is expressed in kg and $T_{p3,SS}$ is expressed in degrees C. Only $T_{p3,SS}$ was a statistically significant variable, with a correlation coefficient of -0.0022, and an adjusted R^2 value of 0.496. The statistical significance of the correlation coefficient between mass yield and $T_{p3,SS}$ indicates that a 95% confidence interval for this value does not include zero, so we are 95% confident that the slope of Equation 5 is non-zero.

$$\hat{Y}_m = 1.282 - 0.0022(T_{p3,SS}) \tag{5}$$

This linear model indicates that as the product 3 steady state temperature increases, on average, the mass yield decreases by 0.22 percentage points per degree Celsius of $T_{p3,SS}$ increase. As with mass yield, the T_p3, SS measurement best described the variation in the energy yield data, with a slope of -0.0018 and an adjusted R^2 of 0.339.

$$\hat{Y}_e = 1.24 - 0.0018(T_{p3,SS}) \tag{6}$$

6. PROXIMATE AND ULTIMATE ANALYSIS

Proximate and ultimate analysis are used to characterize biomass and compare fuels. Proximate analysis typically occurs in a thermogravimetric analyzer (TGA) and measures the moisture content (MC), fixed carbon (FC), volatile matter (VM) and ash (ASH) by mass fraction or percent mass. Ultimate analysis is conducted in a elemental analyzer and measures the content of carbon (C), oxygen (O), hydrogen (H) and sometimes nitrogen (N) and sulfur (S) by mass fraction or percent mass. The characterization of a sample's composition by percent mass of FC, VM and ash, is useful when access to an elemental analyzer, a more specialized instrument, is limited [24, 25].

The proximate analysis results can be used to model ultimate analysis for determining elemental composition, which provides the chemical composition of the product by percent mass of carbon, oxygen, and hydrogen. The mass composition in terms of carbon, oxygen and hydrogen is useful when predicting and modeling the chemical and thermal reactions occurring during torrefaction. This information can be directly used to improve the operation and monitoring of systems for biomass energy generation. For an example, during the combustion of

torrefied biomass in a boiler, this information is useful for operators that do not have access to equipment able to analyze elemental composition of the products [24].

6.1. Analysis of Proximate Data

Proximate analysis was performed on the biomass feedstock and torrefied products and is used to characterize the biomass as a fuel source in regards to torrefaction. Figures 9 and 10 show similar trends; as degree of torrefaction increases, the percent of fixed carbon (FC) increases. In Figure 9, mass yield is the proxy for degree of torrefaction, where, as mass yield decreases, degree of torrefaction increases. In Figure 10, temperature is used as a proxy for degree of torrefaction. Thermocouple product 3, T_{p3}, during steady state was determined to be the best indicator of solid biomass degree of torrefaction. FC can also be used as a proxy for energy content. The increase in FC (by dry weight %) with increasing degree of torrefaction supports the higher energy densities typically found in torrefied products. Most energy is stored in the carbon bonds (FC), however carbon bonds break at a slower rate than bonds to other compounds and, as seen in Figures 9 and 10, carbon is not being released as quickly. There is a moderate to strong liner relationship between FC and degree of torrefaction, where R^2 values for FC versus mass yield and FC versus temperature are 0.7954 and -0.567 respectively (Figures 9 and 10). This means that roughly 80% and 57% of the time, mass yield and temperature respectively can be used to explain percent weight of FC on a dry basis.

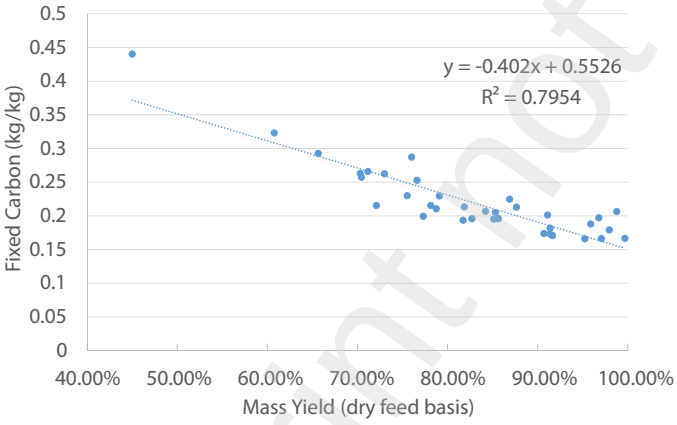

Figure 9: Mass fraction of fixed carbon (FC) from the proximate analysis of the torrefied solid product as a function of mass yield.

The relationship between volatile matter (VM) and the degree of torrefaction is the inverse of that of the FC. The percent of VM (dry weight basis) decreases with degree of torrefaction. In Figures 11 and 12, mass yield and temperature respectively are used as proxies for degree torrefaction. The volatiles are the first constituents to leave the solid product, thus will decrease with degree of torrefaction. There is a moderate to strong liner relationship between VM and degree of torrefaction, where R^2

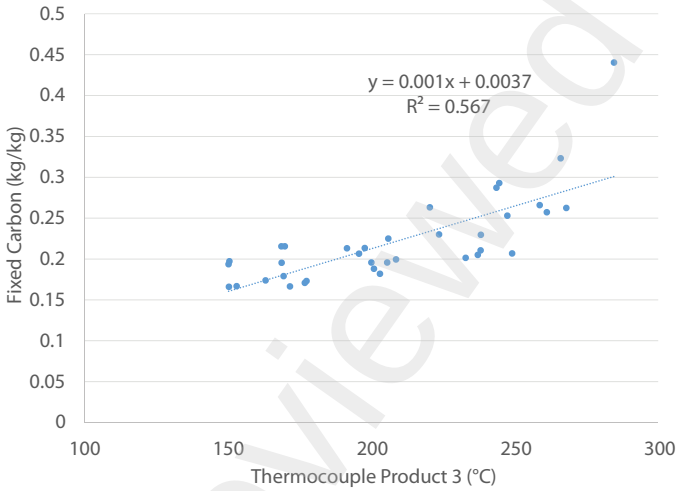

Figure 10: Mass fraction of fixed carbon (FC) from the proximate analysis of the torrefied solid product as a function of temperature. Steady state temperature was measured by thermocouple product 3, as described in Section 4.2.

values for VM versus mass yield and VM versus temperature are 0.6393 and -0.5466 respectively (Figures 11 and 12). This means that roughly 64% and 55% of the time, mass yield and temperature respectively can be used to explain percent weight of VM on a dry basis.

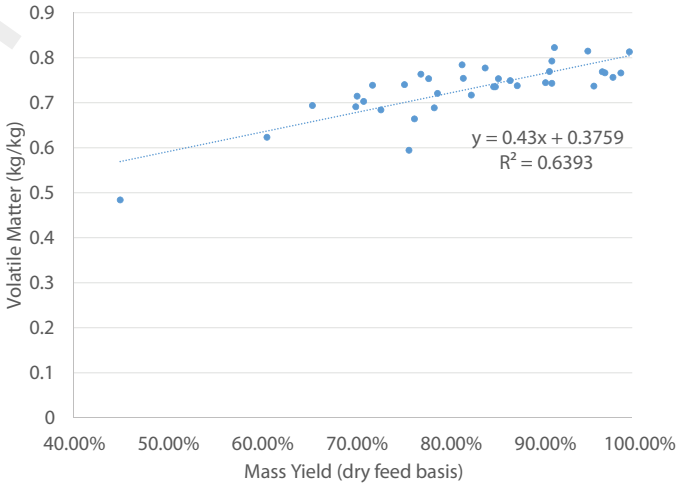

Figure 11: Mass fraction of volatile matter (VM) from the proximate analysis of the torrefied solid product as a function of mass yield.

Unlike FC and VM, ash did not show a linear relationship with degree of torrefaction. Figure 13 presents ash as a function of mass yield as a proxy for degree of torrefaction.

In Figure 14, FC is presented as a function of moisture content (MC), illustrating a weak linear relationship. Given that FC can be used as a proxy for energy content, it can be concluded that energy content does not linearly depend on moisture con-

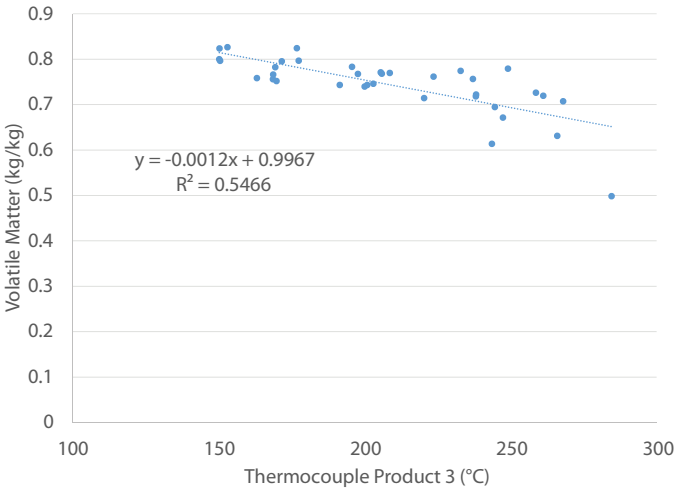

Figure 12: Mass fraction of volatile matter (VM) from the proximate analysis of the torrefied solid product as a function of temperature.

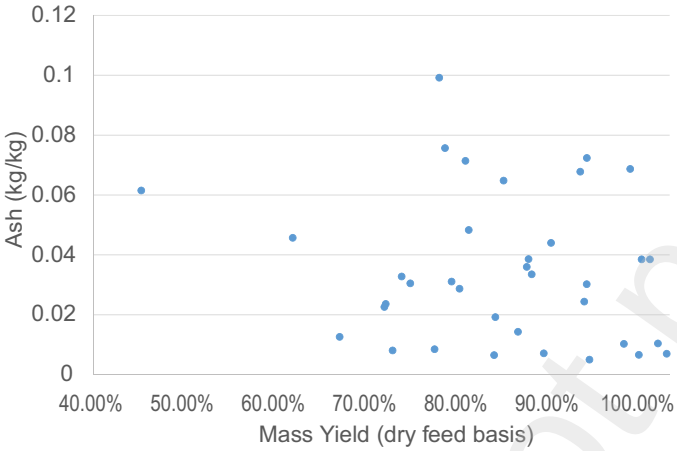

Figure 13: Mass fraction of ash (ASH) from the proximate analysis of the torrefied solid product as a function of mass yield.

tent.

6.2. *Models to Estimate Ultimate Composition*

This section discusses various correlations used to predict ultimate composition from proximate data. Each of the models was used to predict the elemental composition based on the degree of torrefaction or mass yield. The percent weight on a dry basis (percent of weight after moisture content is removed) or mass fractions of the VM, FC, and ash are used to calculate the percent of carbon, hydrogen, and oxygen in each of these models. The same proximate analysis data which was previously analyzed in Section 6.1 will be used in this section.

First, a model was developed by [26], referred to as the 'Parikh model', to predict raw biomass elemental composition through proximate analysis. They gathered 200 samples of biomass species falling into one of the following groups: Pit/Shell/Seeds, Wood/Bark/Energy CropsPruning,

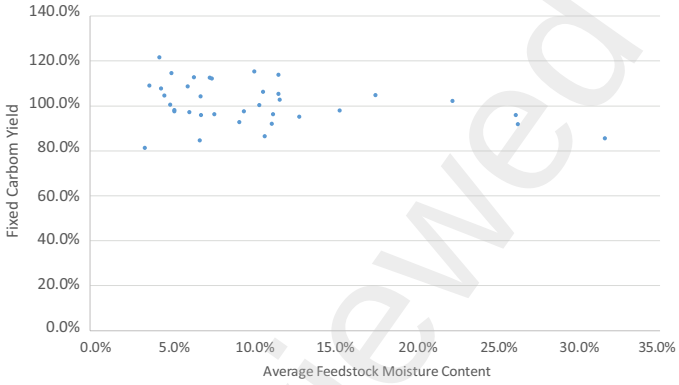

Figure 14: Fixed carbon (FC) (measured in percent dry weight) from the proximate analysis of the torrefied solid product divided by the FC in the feedstock as a function of feedstock moisture content (MC).

Straw/Stalk, Hull/Husk/Dust, and Miscellaneous, and measured proximate data and ultimate composition. They derived a variety of expressions to relate FC and VM from the proximate data to the elemental composition in terms of carbon, hydrogen, and oxygen (by percent weight on dry basis). Model validation was performed with 50 other samples. The final equations for carbon, hydrogen and oxygen are shown in Equations 7-9.

$$C = 0.637(FC) + 0.455(VM) \quad (7)$$

$$H = 0.052(FC) + 0.062(VM) \quad (8)$$

$$O = 0.304(FC) + 0.476(VM) \quad (9)$$

A model was then developed by [25], referred to as the 'Shen' model, using a wide variety of raw biomass proximate and ultimate analysis data, including woods, husks, pits, and trash. They created a ternary model comprised of FC, VM and ash to predict the carbon, hydrogen, and oxygen on a percent dry basis, and determined that models that did not consider ash were inaccurate given the strong effect of temperature on ashing [25]. The Shen model used the least square mean, AAE, and ABE to determine the model that best described the relationship between proximate and ultimate analyses, shown in Equations 10-12.

$$C = 0.635(FC) + 0.460(VM) - 0.095(ASH) \quad (10)$$

$$H = 0.059(FC) + 0.060(VM) + 0.010(ASH) \quad (11)$$

$$O = 0.340(FC) + 469(VM) - 0.023(ASH) \quad (12)$$

Because both the Parikh [26] and Shen [25] models were identified on raw biomass, Nhuchhen [24] considered such models for torrefied products but found large error, thus determining that the current models could not be used to predict elemental composition from proximate analysis for both raw and torrefied biomass [24]. The 'Nhuchhen' model was then devel-

oped using a wide rang of raw and torrefied biomass proximate and ultimate analysis data to find correlations to predict carbon, oxygen and hydrogen mass fractions by using FC, VM and ash. The data used in this model came from more than 40 sources and included hard and soft woods, microalgae and plant husks. Nhuchhen's resulting model is intended for predicting the elemental composition of torrefied biomass but can be used also for raw biomass. However, it is limited to biomass species with low nitrogen contents.

$$C = -35.9972 + 0.7698(VM) + 1.3269(FC) + 0.3250(ASH) \quad (13)$$

$$H = 55.3678 - 0.4830(VM) - 0.5319(FC) - 0.5600(ASH) \quad (14)$$

$$O = 223.6805 - 1.7226(VM) - 2.2296(FC) - 2.2463(ASH) \quad (15)$$

Nhuchhen compared the accuracy of their model for predicting elemental composition for torrefied biomass to the previously discussed Shen and Parikh models, finding that their model is more accurate for torrefied biomass.

In comparing models, for each chemical element, the mean average error (MAE) values are quantified as

$$MAE = \sum_{i=1}^{n} i \frac{|P_i - M_i|}{n}, \quad (16)$$

where P_i is the elemental constituent, M_i is the experimental measured value and n is the number of samples.

For the purpose of this study the Nhuchhen model, with Equations 13-15, is used to predict torrefied biomass elemental composition. Nhuchhen's model used the widest range of both torrefied and raw biomass and was specifically designed to model torrefied biomass composition rather than raw biomass. The model considered the FC, VM and ash components of proximate analysis (rather than just FC and VM like the Parikh model), while also producing the smaller overall model error using mean average error with the Nachenius [14] data.

The Shen model is used to predict the elemental composition of the raw biomass from the proximate analysis. The Shen, Parikh and Nhuchhen models were all used to calculate the elemental composition of the feedstocks. These results are shown in Figure 15. The experimental data in [24] was used again and the model with the smallest mean average error was chosen (Equation 16). The Shen model best predicted the measured values of carbon, hydrogen and oxygen.

Figure 16 is a summary of Figures 9, 11, and 13. The SERC data from this work and the Nachenius [14] measured proximate data exhibit similar trends with degree of torrefaction and mass yield, which is shown in Figure 17. As degree of torrefaction increases (mass yield decreases), the volatile matter mass fraction decreases, the fixed carbon mass fraction increases, and

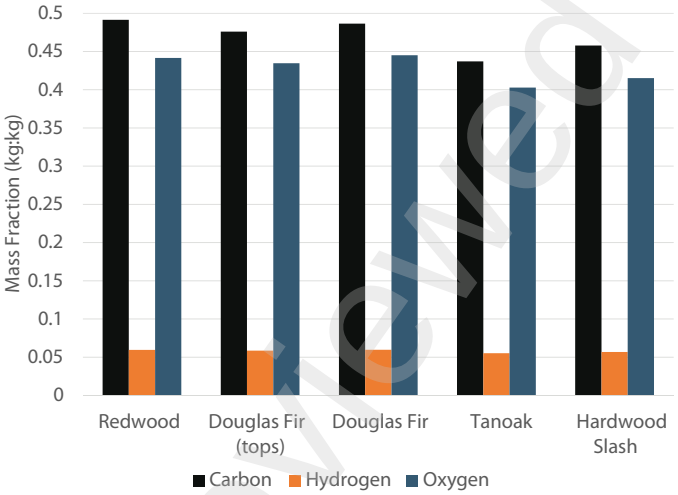

Figure 15: SERC elemental composition by mass fraction of hydrogen, carbon and oxygen of raw biomass sorted by feedstock.

the ash mass fraction stays roughly constant. Linear trendlines are fit to the Nachenius FC and VM data. These trends have R^2 values of 0.981 and 0.9803 for VM and FC respectively. This means that roughly 98% of the variation in VM and FC can be explained by mass yield (a proxy for degree of torrefaction).

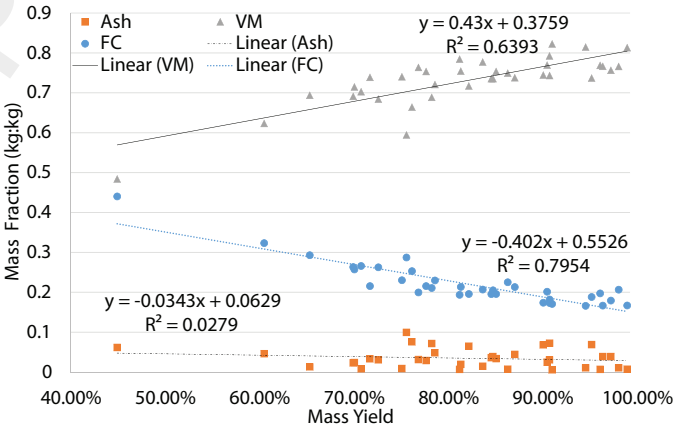

Figure 16: SERC proximate data on a percent dry weight basis including volatile matter (VM), fixed carbon (FC), and ash as a function of mass yield. Linear trendlines are included with the corresponding R^2 values.

The elemental analysis of the SERC biomass using the Nhuchhen model is shown in Figure 18. The trends in hydrogen, carbon, and oxygen percent weight on a dry basis as a function of mass yield are similar to those seen with the Nachenius data. The percent composition of hydrogen is a different order of magnitude to that of the carbon and oxygen. As mass yield decreases, percent of carbon increases, percent of oxygen decreases and percent of hydrogen decreases but with a smaller slope.

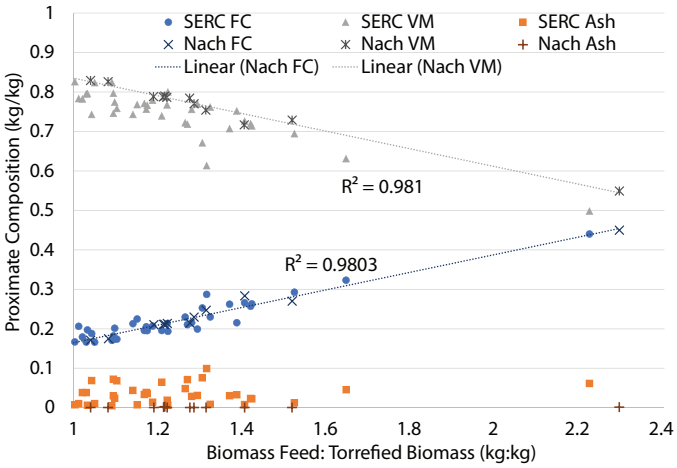

Figure 17: Combined SERC and Nachenius *et al.* (Nach) measured proximate data as a function of 1/mass yield [14]. Volatile matter (VM), fixed carbon (FC), and ash are presented on a dry mass fraction basis. Linear trendlines are included with the corresponding R^2 values.

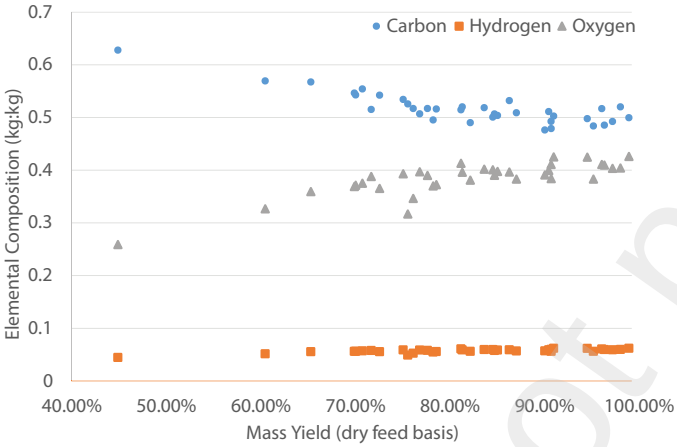

Figure 18: Elemental composition of the SERC torrefied product calculated by using the Nhuchhen model [24]. Carbon (C), hydrogen (H), and oxygen (O) values are presented by mass fraction.

The elemental composition of the SERC data using the Nhuchhen model and the SERC proximate data, it is compared to the Nachenius measured elemental composition (Figure 19). Similar trends are seen between the two models. As degree of torrefaction increases (mass yield decreases), the carbon mass fraction increases, the oxygen mass fraction decreases and the hydrogen mass fraction stays roughly constant.

The oxygen to carbon (O:C) and hydrogen to carbon (H:C) ratios of different biomass species are useful when comparing species behavior during torrefaction. These ratios can be calculated using elemental composition and are used to classify different solid fuels (Figure 20). Nachenius *et al.* extrapolated that with the higher degrees of torrefaction the H:C and O:C ratios approached those of charcoal and coal [14]. The SERC

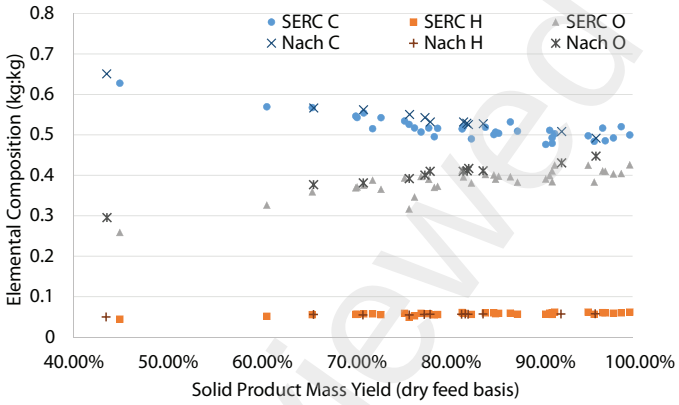

Figure 19: Combined SERC elemental composition data calculated using the Nhuchhen model [24] with experimentally measured Nachenius *et al.* (Nach) elemental composition data. Carbon (C), hydrogen (H), and oxygen (O) values are shown by mass fraction.

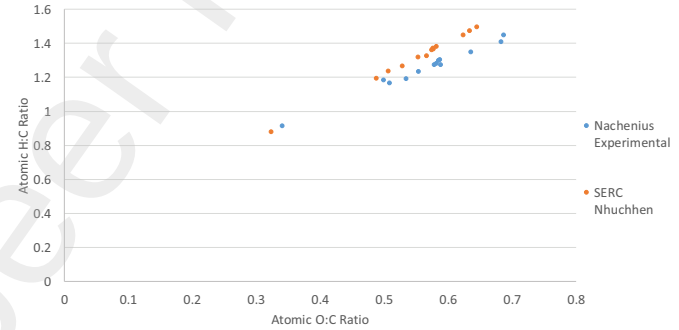

Figure 20: Van Krevelen plot of Nachenius *et al.* and SERC data. H:C and O:C ratios were found using calculated elemental composition data. Van Krevelen plot taken from [14] and overlaid with SERC data.

data is plotted with the Nachenius *et al.* data for reference and a similar linear relationship can be seen in Figure 20.

7. CONCLUSIONS

Several woody species were torrefied in a continuous flow screw torrefier. The mass yield of the torrefied biomass product was considered as a function of residence time, moisture content, feedstock and temperature, both individually and in multiple linear regression. The mass yield exhibited no statistically significant correlations with moisture content, feedstock or residence time. Internal reactor temperatures best predicted the mass yield, with the best predictor being the third product steady state temperature, $T_{p3,SS}$, located at the end of the solid biomass path. The residence time, moisture content and feedstock varieties are parameters which did not influence the final characteristics of the mass yield, used to indicate the torrefaction severity.

Mass yield was shown to be highly correlated with the energy yield, with a similar regression slope as in experimentation per-

formed by [14] and [6]. The energy yield is a linear function of mass yield, and therefore the strong linear correlation is expected between these two variables, however the significant result of this analysis showed that the 95% confidence interval for each linear slope overlapped, indicating that it it possible that the SERC slope is equal to the same value as each of the other models. This finding indicates that the relationship between mass yield and energy yield is consistent between continuous torrefaction reactors of varying sizes with different feedstock inputs.

As mass yield decreases, the fixed carbon percentage in the torrefied product increases, as the volatile matter decreases. The ash content does not change with mass yield to a statistically significant degree.

The proximate analysis is a strong function of mass yield as well as a moderate function of product 3 steady state temperature. The volatile matter decreases with increased degree of torrefaction as the volatile components are vaporized in the torrefier. The fixed carbon increases on a dry mass basis as mass yield decreases, and in runs with internal temperatures over 220^{o}C at the outlet, the fixed carbon yield is greater than 100%, indicating that some volatile matter is converted to fixed carbon, altering the chemical structure of the biomass during torrefaction. The ash content of the torrefied biomass does not depend on the mass yield of the torrefaction experiment.

Elemental composition was predicted for torrefied biomass by the model published by Nhuchhen et al. [24]. As the mass yield decreases, the carbon content of the torrefied product increases, as seen with the fixed carbon content, while the oxygen and hydrogen contents which make up the majority of the volatile matter decrease. For each percentage point decrease in mass yield, the estimated carbon content increased by 0.21 percentage points, while oxygen decreased by 0.22 and hydrogen decreased by only 0.02 percentage points. Increasing degree of torrefaction leads to atomic H/C and O/C ratios increasingly similar in value and ratio to lignite.

References

[1] W.-H. Chen, J. Peng, X. T. Bi, A state-of-the-art review of biomass torrefaction, densification and applications, Renewable and Sustainable Energy Reviews 44 (2015) 847–866.

[2] A. Sharma, V. Pareek, D. Zhang, Biomass pyrolysis—a review of modelling, process parameters and catalytic studies, Renewable and Sustainable Energy Reviews 50 (2015) 1081–1096.

[3] J. Zhao, S. Niu, Y. Li, K. Han, C. Lu, Thermogravimetric analysis and kinetics of combustion of raw and torre ed pine sawdust, Journal of Chemical Engineering of Japan 48 (4) (2015) 320–325.

[4] P. Lv, G. Almeida, P. Perré, Tga-ftir analysis of torrefaction of lignocellulosic components (cellulose, xylan, lignin) in isothermal conditions over a wide range of time durations, BioResources 10 (3) (2015) 4239–4251.

[5] C. J. Roos, Clean heat and power using biomass gasification for industrial and agricultural projects, Tech. rep., Northwest Clean Heat and Power Regional Application Center (2010).

[6] M. Strandberg, I. Olofsson, L. Pommer, S. Wiklund-Lindström, K. Åberg, A. Nordin, Effects of temperature and residence time on continuous torrefaction of spruce wood, Fuel Processing Technology 134 (2015) 387–398.

[7] M. Wilk, A. Magdziarz, I. Kalemba, Characterisation of renewable fuels' torrefaction process with different instrumental techniques, Energy 87 (2015) 259–269.

[8] D. Tapasvi, R. Khalil, Ø. Skreiberg, K.-Q. Tran, M. Grønli, Torrefaction of norwegian birch and spruce: An experimental study using macro-tga, Energy Fuels 26 (2012) 5232–5240.

[9] Y.-H. Kim, B.-I. Na, B.-J. Ahn, H.-W. Lee, J.-W. Lee, Optimal condition of torrefaction for high energy density solid fuel of fast growing tree species, Korean J. Chem. Eng. 32 (8) (2014) 1547–1553.

[10] Y. Joshi, M. D. Marcello, E. Krishnamurthy, W. de Jong, Packed-bed torrefaction of bagasse under inert and oxygenated atmospheres, Energy Fuels 29 (8) (2015) 5078–5087.

[11] J. Chew, V. Doshi, Recent advances in biomass pretreatment – torrefaction fundamentals and technology, Renewable and Sustainable Energy Reviews 15 (2011) 4212–4222.

[12] M. Grigiante, D. Antolini, Mass yield as guide parameter of the torrefaction process. an experimental study of the solid fuel properties referred to two types of biomass, Fuel 153 (2015) 499–509.

[13] J. S. Tumuluru, B. Ghiasi, N. R. Soelberg, S. Sokhansanj, Biomass torrefaction process, product properties, reactor types, and moving bed reactor design concepts, Frontiers in Energy Research 9 (2021) 728140.

[14] R. Nachenius, T. van de Wardt, F. Ronsse, W. Prins, Torrefaction of pine in a bench-scale screw conveyor reactor, Biomass and Bioenergy 79 (2015) 96–104.

[15] L. Shang, J. Ahrenfeldt, J. K. Holm, L. S. Bach, W. Stelte, U. B. Henriksen, Kinetic model for torrefaction of wood chips in a pilot-scale continuous reactor, Journal of Analytical and Applied Pyrolysis 108 (2014) 109–116.

[16] B. Keivani, S. Gultekin, H. Olgun, A. T. Atimtay, Torrefaction of pine wood in a continuous system and optimization of torrefaction conditions, International Journal of Energy Research 42 (15) (2018) 4597–4609.

[17] A. Ohliger, M. Förster, R. Kneer, Torrefaction of beechwood: A parametric study including heat of reaction and grindability, Fuel (2013) 607–613.

[18] D. Chen, D. Liu, H. Zhang, Y. Chen, Effect of torrefaction temperature on biomass pyrolysis using tga and py-gc/ms, in: Asia-Pacific Energy Equipment Engineering Research Conference, Atlantis Press, 2015, pp. 253–256.

[19] H.-S. Han, A. Jacobson, E. M. Bilek, J. Sessions, Waste to wisdom: Utilizing forest residues for the production of bioenergy and biobased products, Applied Engineering in Agriculture, American Society of Agricultural and Biological Engineers 34 (1) (2018) 5–10.

[20] M. A. Severy, C. E. Chamberlin, A. J. Eggink, A. E. Jacobson, Demonstration of a pilot-scale plant for biomass torrefaction and briquetting, Applied Engineering in Agriculture, American Society of Agricultural and Biological Engineers 34 (1) (2018) 85–98.

[21] C. Chamberlin, D. Carter, A. Jacobson, Measuring residence time distributions of wood chips in a screw conveyor reactor, Fuel Processing Technology 178 (2018) 271–282.

[22] I. Casini, D. A. McKahn, Low-order model of the temporal dynamics along the length of a continuous feed biomass torrefier, submitted in review, in: Proceedings of the American Control Conference, 2024.

[23] M. J. C. van der Stelt, Chemistry and reaction kinetics of biowaste torrefaction, Ph.D. thesis, Eindhoven University of Technology (2011).

[24] D. R. Nhuchhen, Prediction of carbon, hydrogen, and oxygen compositions of raw and torrefied biomass using proximate analysis, Fuel 180 (2016) 348–356.

[25] J. Shen, S. Zhu, X. Liu, H. Zhang, J. Tan, The prediction of elemental composition of biomass based on proximate analysis, Energy Conversion and Management 51 (5) (2010) 983–987.

[26] J. Parikh, S. Channiwala, G. Ghosal, A correlation for calculating elemental composition from proximate analysis of biomass materials, Fuel 86 (2007) 1710–1719.